ISSN: 0975-833X

Available online at http://www.journalcra.com

INTERNATIONAL JOURNAL OF CURRENT RESEARCH

International Journal of Current Research
Vol. 14, Issue, 03, pp.20985-20988, March, 2022

DOI: https://doi.org/10.24941/ijcr.43259.03.2022

RESEARCH ARTICLE

ELECTROMAGNETIC WAVE PROPAGATION IN A SEA SURFACE COVERED BY FOAM USING SPLIT-STEP FOURIER TRANSFORM AT WIND SAT FREQUENCIES.

[1]Aguiyi Nduka Watson and [2]Ayibapreye K. Benjamin

[1]Department of Electrical, Electronic Engineering, Federal University Otueke
[2]Department of Electrical, Electronic Engineering, Niger Delta University

ARTICLE INFO

Article History:
Received 24th December, 2021
Received in revised form
19th January, 2022
Accepted 24th February, 2022
Published online 30th March, 2022

Keywords:

Electromagnetic Wave,
sea-foam, Sea-Surface,
Split-step Fourier Transform,
WindSat.

Corresponding author:
Ayibapreye K. Benjamin

ABSTRACT

Electromagnetic (EM) wave propagationthrough a physical model of foam-covered sea surface modelled as layers of randomly distributed air-bubbles coated with thin layer of sea water was investigated. Here, the matching potential of the split-step Fourier technique was explored by slicing the three-dimension $(3D)$ foam structure into two-dimension $(2D)$ layers and determine the vertical field profiles of the propagating E-field at successive range steps until the desired range is reached. The scatterer (foam layer) comprises of randomly distributed packed bubbles with estimated complex dielectric constant of sea foam which is a mixture of air coated with thin layer of sea water. It has internal and external radii r_{in} and r_o. The bubble size distribution $N(r)$ follows a log-normal distribution pattern. We consider a cluster of N bubbles randomly packed closely such that there exists no overlap between any two adjacent bubbles. The bubbles are assumed to be spherical in shape and are placed in a finite domain in the form of a cube with dimensions $L(length) = B(width) = H(height)$. The sea foam model is described by three regions embedded in inequality $0 \leq z \leq d$, the incident field $u(z,x,y)$ must satisfy the Helmholtz equation. Results of EM field intensity through layers of sea foams as at selected WindSat frequencies were reported.

Citation: Aguiyi Nduka Watson and Ayibapreye K. Benjamin. "Electromagnetic wave propagation in a sea surface covered by foam using split-step fourier transform at wind sat frequencies", *2022. International Journal of Current Research, 14, (03), 20985-20988.*

INTRODUCTION

Earlier reports asserted that sea foam presence in seawater greatly enhances thermal emission from the ocean surface (1, 2, 3, 4). Foam generated by breaking waves under strong wind conditions have significant effect on the average brightness of the ocean (8). Which is an attribute of thermal radiation by cloud and scattering of this radiation by the sea surface affects the effective brightness temperature observed by satellite radiometers. Hence, ignoring specular reflections from cloud which radiates on the foam-covered sea surface leads to inaccurate estimate of sea surface emissivity. Due to the important role sea foam plays in passive microwave remote sensing, there is need to provide an accurate estimate of thermal emission from foam covered sea surface at microwave frequencies. However, little theoretical progress has been made on the accurate modeling and understanding of sea foam emission since the 1970s.

Important early contributions include the work by Droppleman (5), who modelled the foam as a homogeneous effective medium with mixture of air and water and found that the emissivity approached one for high air fraction. Rosenkranz and Staelin (6) constructed a more elaborate model where the foam layer is approximated by thin parallel layers of water separated by air. Even though these models could explain the high emissivity from sea foam, they were rather idealized and did not relate to the under- lying physical parameters of the foam. On the other hand, recent studies of thermal emission from the ocean surface have focused on incorporating rough surface effects (7, 8). To take into account of emission from foam, one usually has to resort to an empirical formula (9). The aforementioned challenge inspired the need to develop a physical based foam model that accounts for foam micro-structure and foam layer thickness.

In this paper, the foam was modelled as a layer of randomly distributed air bubbles overlying a flat ocean (Figure 1). It was assumed that air bubbles are spherical in shape and covered with thin layer of seawater. The optical properties of sea foam, mainly the effective dielectric constant of the lower half-space and water shell is expressed as , while the effective dielectric constant inside and outside the shell is. Zhang (10) reported similar foam model using Rayleigh scattering and the independent scattering approximation. Thereby, limiting its validity to small bubbles that are sparsely distributed. Sea foam bubbles dependence on wind speeds and stages of development makes it to come in a variety of sizes as well as densities. Hence, the need to consider the general case of bubbles been closely packed with sizes comparable to the wavelength of incident electromagnetic field. Remote sensing of sea foams was investigated by application of these parameters as inputs for radiative transfer calculations. In practice, actual wind driven ocean surface appears rough. Here, it was assumed that the ocean surface is flat in order to evaluate the attenuation of the E-fields in slices of foam layer. Large scale surface roughness in the ocean can be accounted for using geometric tilting model. This model relates emission from a tilted foam layer to emission from a flat foam layer by polarization transformations and emission from a flat foam layer through simple angle. We are focused on evaluation of the EM wave perturbation from flat sea surface covered by random bubble scatterers. Here, atmospheric effects are neglected though important in passive remote sensing of the ocean.

We adapt an analytical and theoretical model of flat sea-surface covered by foam which is modelled as randomly distributed air-bubbles that are log-normally distributed. The foam is described as air entrapped in thin layer of seawater. This is significant for accurate computation of ocean brightness temperatures. The sea surface emissivity in the presence of foam in seawater helps to ensure accurate evaluation of ocean brightness temperatures which were not accounted for using empirical methods. By adopting mechanical and optical properties of foam such as foam layer thickness, bubble size distribution, foam void fraction, effective dielectric constants of randomly distributed bubbles and sea surface temperature, thermal emission from the ocean surface covered by foam can be evaluated.

Problem Formulation: The adopted approach models sea foam to account for the optical and geometrical properties such as foam layer thickness, foam void fraction, bubble radii, bubble size distribution (BSD), and bubble shape. BSD and bubble radii are computed by inverse cumulative error function using Newton Raphson method. Random sphere close packing is applied for filling the bubbles in three-dimensional) domain. The domain could be cube, cuboid, prism, or cylinder but a cubic domain was assumed for simplicity as we in- tend to divide the domain into slices of domain. The packing of air-bubbles or spheres is done such that no two adjacent bubbles overlap. For irregular distribution of air-bubbles (foams), the random close packing is used to achieve a densely packing with bubble volume fraction of with the within the host domain having a geometry of for maximum packing density. In this approach the air-bubbles locations or positions were generated using uniformly distributed random numbers in ,and coordinates. Computation of bubble radii for n-randomly distributed bubbles were done in FORTRAN 90 complier using inverse method.

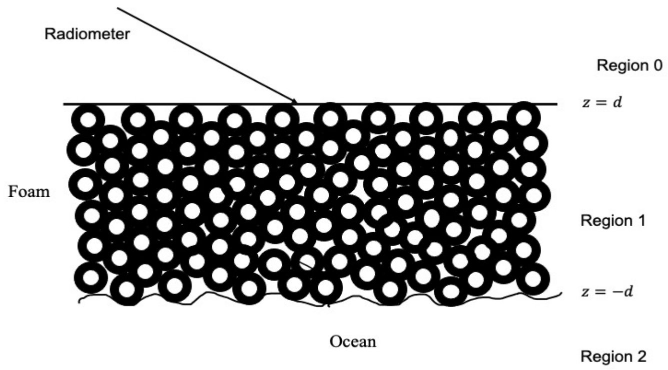

Figure 1: Diagrammatic representation of foam-covered ocean surface showing three different regions

The inverse method transforms uniform variate $U(0,1)$ to normal variate $N(0,1)$. BSD $N(r)$ and bubble radii $r_i$were computed with mean $\mu = 2.0$ and standard deviation $\sigma = 0.5$, geometric mean $\mu_g = 500$ micron and geometric standard deviation $\sigma_g = 2.0$. This was implemented using an empirical expression for the scaled normal variate and log-normally distributed BSD. The Split-step approximation was adopted for evaluation of thermal emission in the foam layered sea surface. The Split- step Fourier method is a range marching technique efficient for prediction of field perturbations at each slice of foam layer. Hence, the need to translate 3-D to 2-D slices.

Split-step Fourier Transform: The split-step Fourier method is a very efficient PEM which separate the refractive effect from the diffractive part of the propagator. Considering a two-dimensional scalar wave equation for horizontally and vertically polarised wave. Hardin et.al introduced the split-step Fourier method which transforms the rough surface problem with propagation through a sequence of phase screens (11).

The standard parabolic equation (SPE) can be written as

$$\frac{\partial u}{\partial x} = \frac{ik}{2}\left\{\frac{1}{k^2}\frac{\partial^2}{\partial z^2} + (n^2(x,z) - 1)\right\}u \quad (1)$$

Let $A = \frac{1}{k^2}\frac{\partial^2}{\partial z^2}$ (2)

$$B = n^2(x,z) - 1 \quad (3)$$

Equation (1.44) becomes

$$\frac{\partial u}{\partial x} = \frac{ik}{2}\{A + B\}u \quad (4)$$

The analytic solution of the SPE is $u(x + \Delta x, z) = u(x,z)e^{\frac{ik}{2}\Delta x(A+B)}$ (5)

Using

$$\delta = \frac{ik\Delta x}{2} \quad (6)$$

Equation (5) yields

$$u(x + \Delta x, z) = u(x,z)e^{\delta(A+B)} \quad (7)$$

Equation (5) is the split-step solution which represent the field propagating through series of phase screens. The field is first propagated through a slice of homogeneous medium characterised by the exponent of A. The numerical split-step parabolic solution for $j = 1,2 \ldots M$ is given as

$$u(x_0 + \Delta x, z) = \exp\left[i\frac{k_0}{2}(-1)\Delta x\right]$$

$$F^{-1}\left[\exp\left(-i\frac{p^2\Delta x}{2k_0}\right)\right] F(u(x_0 + (j-1)\Delta x, z)) \qquad (8)$$

This equation can be used to calculate $u(x,z)$ along z with steps of Δx, for known initial source distribution $u(0,z)$. We can use a 1-D array to store the transverse field profiles of Nx vertical height points and Nz discrete ranges, with replacement. Here, the initial field $u(0,z)$ profile obtained from an antenna beam pattern is propagated along x-direction from x_0 to Δx for $j = 1$ using equation (8) until the solution $u(x_0 + \Delta x, z)$ is obtained. This process is repeated for $j = 1,2 \ldots\ldots M$, the field solution for $j = 2$ is used as the initial field for $u(x_0 + 2\Delta x, z)$ and the vertical field profiles are computed for each range step until the desired range is reached (12-13).

RESULTS AND DISCUSSION

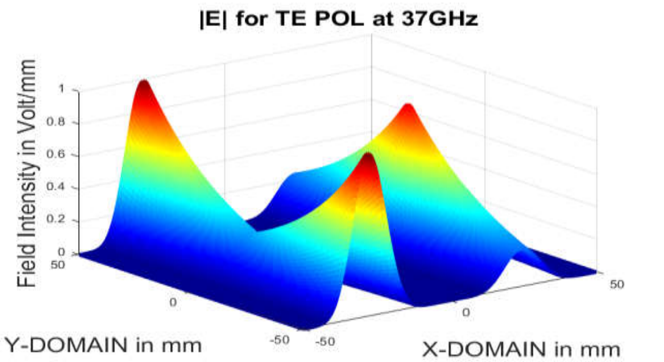

Figure 2: Field intensity of backscattered wave for horizontal polarization (TE) with zenith $\theta_i = 30^\circ$ and azimuth $\varphi = 0^\circ$ as a function of the spatial coordinates X and Y of the propagation media at 37 GHz and $\delta_t = 2\,mm$. The amplitude of the E-field attenuates as it propagates through successive layers of seafoam. The diffractive factor of the split-step propagator $exp(i\Delta x\sqrt{k^2 - (p^2 + q^2)}$ accounts for the attenuation of the E-field as it travels through the 5 slices of seafoam layers. The field intensity of the scattered E-field at various WindSat frequencies shows that attenuation increase with increasing depth of the seafoam slices.

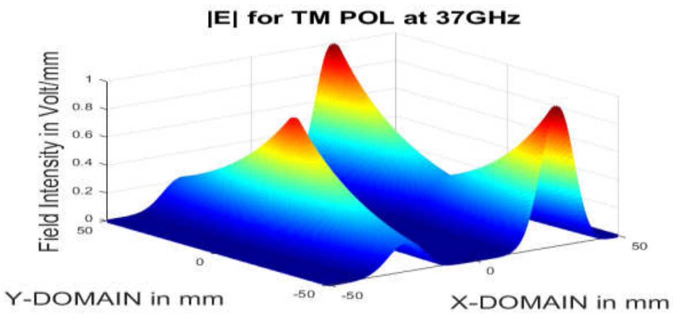

Figure 3: Field intensity of backscattered wave for vertical polarization (TM) with zenith $\theta_i = 30^\circ$ and azimuth $\varphi = 0^\circ$ as a function of the spatial coordinates X and Y of the propagation media at 37 GHz and $\delta_t = 2\,mm$.

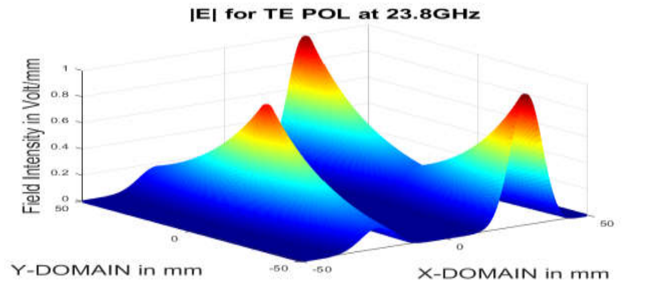

Figure 4: Field intensity of backscattered wave for horizontal polarization (TE) with zenith $\theta_i = 30^\circ$ and azimuth $\varphi = 0^\circ$ as a function of the spatial coordinates X and Y of the propagation media at 23.8 GHz and $\delta_t = 2\,mm$.

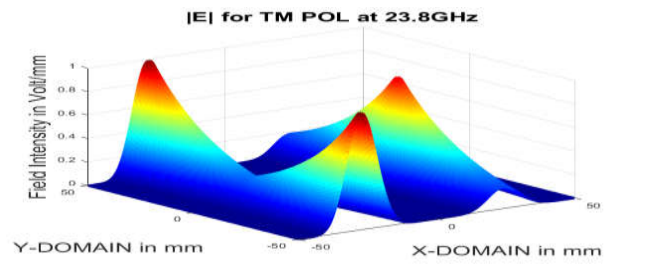

Figure 5: Field intensity of backscattered wave for vertical polarization (TM) with zenith $\theta_i = 30^\circ$ and azimuth $\varphi = 0^\circ$ as a function of the spatial coordinates X and Y of the propagation media at 23.8 GHz and $\delta_t = 2\,mm$.

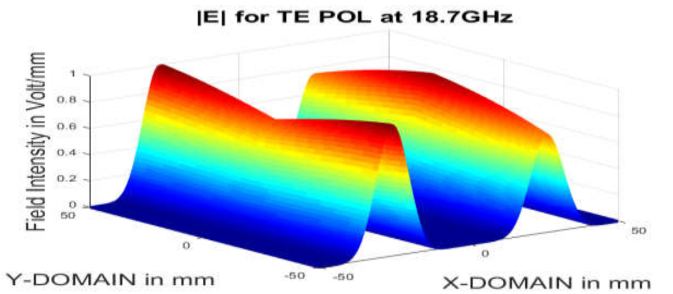

Figure 6: Field intensity of backscattered wave for horizontal polarization (TE) with zenith $\theta_i = 30^\circ$ and azimuth $\varphi = 0^\circ$ as a function of the spatial coordinates X and Y of the propagation media at 18.7 GHz and $\delta_t = 2\,mm$.

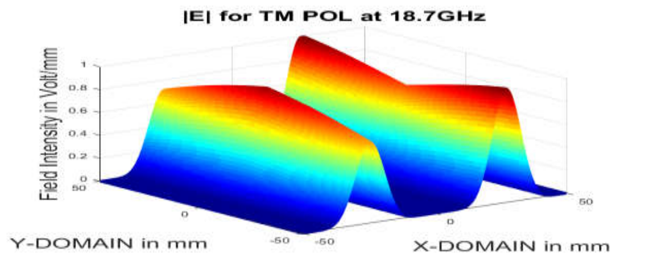

Figure7: Field intensity of backscattered wave for vertical polarization (TM) with zenith $\theta_i = 30^\circ$ and azimuth $\varphi = 0^\circ$ as a function of the spatial coordinates X and Y of the propagation media at 18.7 GHz and $\delta_t = 2\,mm$.

The amplitude of the E-field varies with angular wave-number in radians as it propagates through slices of the sea foam layer. Figures above illustrates variation of field intensity of the E-field for both TE and TM polarizations with spatial domains which describe attenuation of the propagated E-field along the spatial directions. We can see the fluctuation in peaks of the diffracted E-field is due to the random varying effective dielectric constants of sea-foam with varying size distributions. Plane waves attenuate as they propagate through a lossy medium. From the expression of skin depth, it is found that the depth of penetration of fields in a lossy medium is inversely proportional to the square-root of the conductivity of the medium. In the extreme case of conductivity close to infinity, this depth vanishes and in fact, time varying fields and induced currents cannot exist within the medium. In other words, all fields and induced currents are confined near the skin region of the medium. We observed that an increased high frequency resistance of a thin sea-foam layer, which occurs as a result of current confinement through a smaller cross-section due to the skin effect.

In the ocean (seawater) with loss tangent greater than unity, we observe that attenuation of the E-field increased with depth. Antennas used for transmitting and receiving EM waves will cover more distance at lower propagating frequencies as the depth of penetration is inversely proportional to the attenuation constant. Attenuation is proportional to the square-root of the radian frequency in a lossy medium. We have shown that the amplitude of the E-field attenuates with depth of seafoam slices with exception to the scenario where the wave field is absorbed for large seafoam slice thickness $\delta_t = 2\,mm$. It was apparent that this phenomenon is true for all WindSat frequency channels. We can conclude that the amplitude of the E-field attenuates with increase in frequency and depth of seafoam slice thicknesses.

CONCLUSION

In this investigation, the presence of sea foams on the ocean surface causes attenuation of the EM waves due to diffuse scattering when the incident E-field is multiple reflected by sea-foam as it propagates through the various slices of sea-foam layer. The split-step Fourier transform method as a range marching is suitable for evaluation of the E-field propagation given an initial range, the expected depth of the field can be computed as a function of range and depth. The E-field propagates through different paths and is scattered due to re-radiation of the dipole moments of the disoriented scatterers which absorbs some of the incident E-field and re-radiates it at various directions. The varying effective dielectric constants of the particles enhances diffuse scattering of the incident and transmitted E-fields within the sea-foam layer.

REFERENCES

(1) Williams, G.F. “Microwave radiometry of the ocean and the possibility of marine wind velocity determination from satellite observations,” J. Geophys. Res., vol. 74, no. 18, pp. 4591–4594, 1969.

(2) Hollinger, J. “Passive microwave measurements of the sea surface,” J. Geophys. Res., vol. 75, no. 27, pp. 5209–5213, 1970.

(3) Nordberg, W. J. Conaway, D. Ross, and T. Wilheit, “Measurements of microwave emission from a foam covered, wind driven sea,” J. Atmos. Sci., vol. 28, pp. 429–435, 1971.

(4) Smith, P.M. “Theemissivityofseafoamat19and37GHz,” IEEE Trans. Geosci. Remote Sensing, vol. 26, no. 5, pp. 541–547, Sep. 1988.

(5) Droppleman, J. D. “Apparent microwave emissivity of sea foam,” J. Geophys. Res., vol. 75, no. 3, pp. 696–698, Jan. 1970.

(6) Rosenkranz P.W. and Staelin, D.H. “Microwave emissivity of ocean foam and its effect on nadiral radiometric measurements,” J. Geophys. Res., vol. 77, no. 33, pp. 6528–6538, Nov. 1972.

(7) Kunkeeand D.B. A.J. Gasiewski, “Simulation of passive microwave wind direction signatures over the ocean using an asymmetric-wave geometrical optics model,” Radio Sci., vol. 32, no. 1, pp. 59–78, Jan.–Feb. 1997.

(8) Yueh, S. H. “Modeling of wind direction signals in polarimetric sea surface brightness temperatures,” IEEE Trans. Geosci. Remote Sensing, vol. 35, no. 6, pp. 1400–1418, Nov. 1997.

(9) Stogryn, A. “The emissivity of sea foam at microwave frequencies,” J. Geophys. Res., vol. 77, no. 9, pp. 1658–1666, Mar. 1972.

(10) Zhang, Y. Forward and Inverse Problems in Microwave Remote Sensing of Objects in a Complex Medium, Ph.D. thesis, Massachusetts Institute of Technology, 1999.

(11) Benjamin A. and D. O. Bebbington, “Millimeter wave propagation and attenuation in closed packed sea foam layer and complex dielectric constant of sea-foam using split-step Fourier transform”, *Progress in Electromagnetic Symposium-Fall (PIERS-FALL), IEEE*, 2556-2553, 2017.

(12) Benjamin A. K. and C. E. Ouserigha. "Extinction of Millimeter wave on Two Dimensional Slices of Foam-Covered Sea-surface.", International Journal of Scientific Research and Engineering Development, vol. 3, no. 4, July-August 2020.

(13) Benjamin, A.K., 2019. *Evaluation of millimetre-wave coherent scattering from a sea surface covered by foam modelled as sequences of thin phase-scattering screens using split-step Fourier method* (Doctoral dissertation, University of Essex).

****